

Therefore, it has to be concluded that judgement of the validity of the approximation at u_1 equal to one r.m.s.d. is not sufficient. An interval of at least three times the r.m.s.d. should be taken into consideration.

If large anharmonic effects are supposed, even greater regions in \mathbf{u} have to be considered, because of the deformation of the normal distribution of the harmonic p.d.f.

Acta Cryst. (1988). **A44**, 558–562

Determination of Structure-Factor Phase Invariants and Effective Structure Factors in Non-centrosymmetric Crystals

BY KNUT MARTHINSEN* AND RAGNVALD HØIER

Department of Physics and Mathematics, University of Trondheim-NTH, N-7034 Trondheim, Norway

(Received 14 December 1987; accepted 11 March 1988)

Abstract

Many-beam diffraction effects in non-centrosymmetric crystals have been studied with emphasis on three-beam interactions and determination of three-phase structure invariants in electron diffraction experiments. The effective structure factor has been determined both by numerical many-beam calculations and from the second Bethe approximation. The dependence of this factor on the phase invariant, the excitation errors and the magnitude of the structure factors involved has been discussed in detail. From the values of the effective structure factors at symmetrical positions on each side of a three-beam condition an asymmetry ratio is introduced. By a comparison of the observed variation in this ratio with theoretical profiles, it has been shown that the magnitude of three-phase invariants can be determined in the non-centrosymmetric case. This method may in principle be applied in any type of electron or X-ray three-beam experiments where variations in the effective structure factor are projected out. An example from electron channelling patterns is given.

Introduction

The structure-factor phase problem is central in all crystallographic diffraction studies, and various methods are used to handle it. In X-ray structure determination using direct methods phases are usually estimated with some probability by statistical methods from relations between structure-factor

- References**
- MATSUBARA, T. (1975). *Prog. Theor. Phys.* **53**, 1210–1211.
 MERISALO, M. & LARSEN, F. K. (1977). *Acta Cryst.* **A33**, 351–354.
 MERISALO, M. & LARSEN, F. K. (1979). *Acta Cryst.* **A35**, 325–327.
 ROSSMANITH, E. (1984). *Acta Cryst.* **B40**, 244–249.
 TANAKA, K. & MARUMO, F. (1983). *Acta Cryst.* **A39**, 631–641.
 WILLIS, B. T. M. (1969). *Acta Cryst.* **A25**, 277–300.
 WILLIS, B. T. M. & PRYOR, A. W. (1975). *Thermal Vibrations in Crystallography*. Cambridge Univ. Press.
 ZUCKER, U. H. & SCHULZ, H. (1982). *Acta Cryst.* **A38**, 563–568.

amplitudes (e.g. Woolfson, 1987). One direct way, however, to solve the problem is to utilize the intensity anomalies observed in dynamical many-beam diffraction experiments. Here additional information is available compared with standard experiments. This concerns in principle both the magnitudes of the structure factors and the three-phase structure invariants.

In many-beam investigations a perturbed two-beam, or two-Bloch-wave, point of view has often proved to be successful. On this basis the effective structure factor has been introduced, and a theoretical background for obtaining structure-factor phase information has been established. It is clear that three-phase invariants, in principle, can be determined from any type of electron or X-ray three-beam experiment where the effective structure factor, i.e. the effective dispersion surface gap width, is projected out. In practice this possibility is now well established for the centrosymmetric case.

Dependence of the observed intensity anomalies on the various parameters in mainly centrosymmetric crystals has been discussed in non-systematic many-beam electron diffraction cases by, for example, Kambe (1957), Gjønnes & Høier (1971), Gjønnes (1981) and Marthinsen & Høier (1986). The X-ray case has been discussed by Post (1979, 1983), Chapman, Yoder & Colella (1981), Marthinsen (1981), Thorkildsen & Mo (1982), Chang (1982, 1986), Juretschke (1982, 1986), Hümmer & Billy (1982, 1986), Høier & Marthinsen (1983), Thorkildsen (1987) and Marthinsen & Høier (1987).

In the present studies we shall focus on the determination of effective structure factors and a new method

* Present address: SINTEF, Division of Applied Physics, N-7034 Trondheim, Norway.

to determine structure-factor phase invariants. Centrosymmetric crystals have been studied in some detail previously. In the present investigation we shall therefore concentrate on the general non-centrosymmetric case. Some results have been given previously by Marthinsen, Matsuhata, Høier & Gjønnes (1987).

Theory

A general three-beam case is shown schematically in Fig. 1, where the straight lines h and g represent the zone boundaries for the reflections h and g . The kinematical condition of simultaneous Bragg reflection corresponds to the position T , which is the centre of the Ewald sphere projected on the reciprocal plane. The deviation from the Bragg condition, the excitation errors s_h and s_g , is linearly dependent on the parameters x and y which determine the position $\mathbf{r}(x, y)$ of the projected Ewald-sphere centre in the general case:

$$ks_g = \mathbf{r} \cdot \mathbf{g}. \quad (1)$$

Here k is the wave vector and \mathbf{g} the reciprocal-lattice vector for the reflection g .

The geometric positions of the Bragg condition in both the kinematic and the two-beam cases are thus represented by the straight lines. They also represent the projection on the reciprocal plane of the position of the two-beam dispersion surface gap, *i.e.* the position where the distance between the two dispersion-surface sheets has its minimum value and consequently the Bragg scattering its maximum value.

When three beams or more are present simultaneously, the particular incident-beam direction which corresponds to minimum distance between the two dispersion-surface sheets also excited in the two-beam case, and hence maximum Bragg scattering in this case, is displaced from the two-beam direction. Projected on the reciprocal plane, the positions of the perturbed two-beam gaps will, in the three-beam case, be along the two hyperbolae shown schemati-

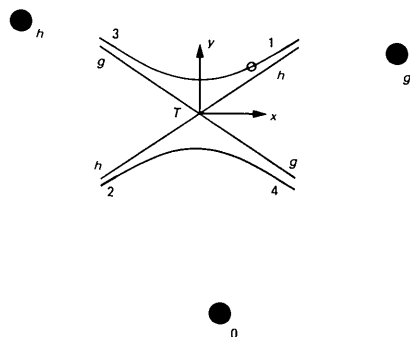


Fig. 1. 0, h , g three-beam case. Dispersion-surface gap positions projected on reciprocal plane (not to scale). The small circle on branch 1 indicates the position of minimum dispersion-surface gap width.

Table 1. Structure factors U_h for electron diffraction in GaP at 40 kV

Reflection	hkl	$ U_{hkl} $ (\AA^{-2})	φ_{hkl} ($^\circ$)
g	3 $\bar{5}$ 1	0.42	-27
h	4 $\bar{4}$ $\bar{2}$	0.17	0
$g-h$	$\bar{1}$ 1 3	0.95	34

cally in Fig. 1. At one particular position, indicated with a circle, the perturbed gap width associated with the weaker h beam may have a minimum. For centrosymmetric crystals this position corresponds to the critical direction degeneracy discussed by Gjønnes & Høier (1971).

The magnitude of the effective structure factor, $|U_h^{\text{eff}}|$, is now defined from the calculated perturbed two-beam gap width which shall be determined numerically from full many-beam calculations using three or more beams. For comparison, calculations based on the Bethe approximation are included. This analytical expression, which includes explicitly the most important parameter dependences to be expected in the full calculations as well, may be written for the weak h beam in the three-beam case as

$$|U_h^{\text{eff}}| = |U_h| \left[\left(1 - \frac{|U_g| |U_{h-g}|}{|U_h| 2ks_g} \cos \psi \right)^2 + \left(\frac{|U_g| |U_{h-g}|}{|U_h| 2ks_g} \right)^2 \sin^2 \psi \right]^{1/2}. \quad (2)$$

The generalization to further interacting beams g is straightforward. In the equation the excitation error s_g of the coupled beam is defined negative when the reciprocal-lattice point g is outside the Ewald sphere. The quantity ψ is the three-phase structure invariant

$$\psi = \varphi_{-g} + \varphi_h + \varphi_{g-h}. \quad (3)$$

Here φ_h is the phase of the structure factor, *i.e.* $U_h = |U_h| \exp(i\varphi_h)$.

Calculations

In the calculations we shall use an example from GaP. Data for the structure factors, *i.e.* the Fourier coefficients of the potential, are given in Table 1.

From the data in Table 1 the three-phase invariant in this case is seen to be $\psi = 61^\circ$.

As in the standard theory (*e.g.* Humphreys, 1979), a cut through the three-beam dispersion surface, defined by the *Anpassungen* γ^j , is now calculated numerically for each value of x by varying the parameter y in Fig. 1, using (1) to determine s_g and s_h . In this way the position of the dispersion-surface gap as well as the gap width are determined. The section for constant x going along the line a in Fig. 5 (*i.e.* close to the minimum-gap position in Fig. 1) is shown in Fig. 2. This section corresponds to going from a one-beam case (no diffraction) through a three-beam

case slightly off the exact three-beam condition (the distance $x = a$) and then back to a one-beam case again. In this figure the dashed straight lines indicate the surfaces of the spheres around each reciprocal-lattice point, and the bars at the bottom show by their positions and lengths the two-beam positions and gap widths, respectively. The gap to the left, which corresponds to the g beam, is enhanced relative to the two-beam value. The other gap corresponds to the weakened h beam.

The gap positions are found to be located in the projection as shown schematically in Fig. 1. Segments 1 and 2 correspond to the new displaced Bragg positions of the weaker of the two reflections, h , and segments 3 and 4 to the stronger one, g .

The effective structure factor given by the calculated gap width along the h segments 1 and 2 in Fig. 1 is shown in Fig. 3(a) as a function of the deviation parameter x . In addition to the actual case with ψ equal to 61° the phases have been varied as shown. The magnitudes of the three structure factors involved have been kept constant.

For negative x Fig. 3(a) shows that $|U_h^{\text{eff}}|$ increases continuously with increasing x and increases when the phase invariant decreases from 90° to 0 .

For positive x and small values of the invariant, $|U_h^{\text{eff}}|$ first decreases and then increases towards the two-beam value for increasing x . When the phase invariant is larger, the minimum is less pronounced and almost unobservable at $\psi = 61^\circ$. For $\psi = 0^\circ$ the gap is zero for a particular x (and y) value in agreement with the analytical solutions found by Gjønnes & Høier (1971) for this case. These solutions also show that the x, y set have opposite sign when $\psi = 180^\circ$. It should also be noticed that the effective structure factor is symmetric in x when $\psi = 90^\circ$.

Based on Fig. 3 we now define the effective structure-factor asymmetry ratio η by the values at x and $-x$, *i.e.*

$$\eta = \frac{|U_h^{\text{eff}}(x < 0)|}{|U_h^{\text{eff}}(-x)|}. \quad (4)$$

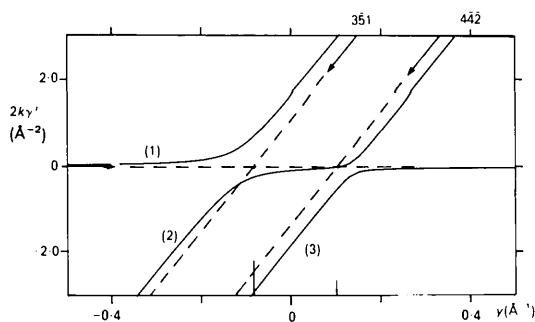


Fig. 2. Calculated dispersion surface as a function of y for the 000, 351, 442 three-beam case in GaP corresponding to section a in Fig. 5(a).

The calculated variation in this quantity with the diffraction condition is shown in Fig. 4(a). An analogous ratio based on Bethe intensities has previously been introduced by Juretschke (1982). However, the asymmetry ratio defined here, based on effective structure factors, is more general in that it may be extracted from any type of three-beam experiment where variations in the effective structure factor somehow project out. The ratio in (4) is seen from the figure to be strongly dependent on the phase invariant. It diverges for a particular x value when $\psi = 0^\circ$ and is constant for $\psi = 90^\circ$. It should here be stressed that the inverse ratios are found for negative values of the cosine term in (2).

Fig. 4(a) shows the variation in the weaker of the two Bragg beams, h , while (b) shows the stronger one, g . It is clear that the strongest variation will be found in the h reflection. This agrees with the approximate solution given in (2). Here one of the important parameters for the perturbation of the weakest beam, h , is the structure-factor product $|U_g||U_{h-g}|/|U_h|$. This product is 2.3 \AA^{-2} in Fig. 4(a) and 0.4 \AA^{-2} in Fig. 4(b). With decreasing structure-factor product the effect hence decreases and the position of the

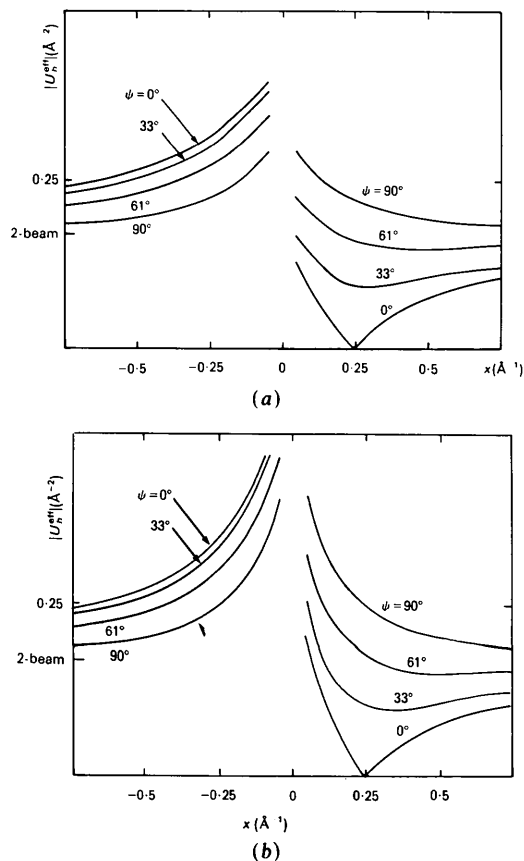
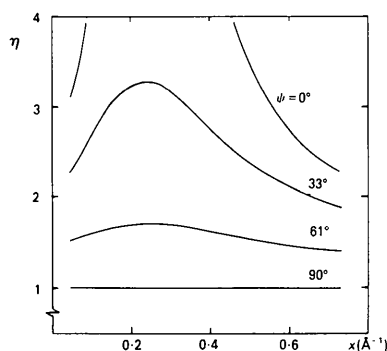


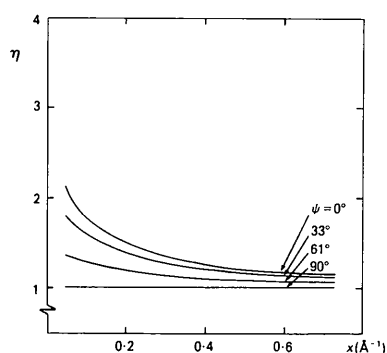
Fig. 3. Variation in the effective structure factor, $|U_h^{\text{eff}}|$, with the deviation parameter and the three-phase structure invariant. (a) Full three-beam calculations. (b) Calculations based on the second Bethe approximation.

maximum structure-factor asymmetry ratio moves towards smaller x values.

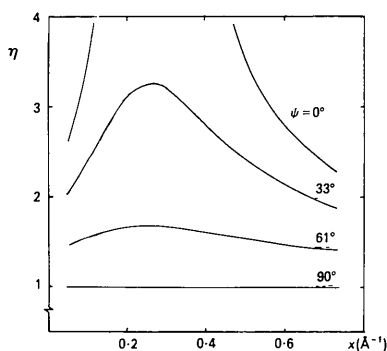
To investigate the validity of the second Bethe approximation in this connection, the effective structure factor has been calculated for the same case as the one above. The results for the weak beam are shown in Fig. 3(b). The corresponding variation in the asymmetry ratio shown in Fig. 4(c) is in principle similar to the Bethe-intensity results of Juretschke



(a)



(b)



(c)

Fig. 4. Calculated asymmetry ratio η as a function of the deviation parameter x . (a) Full three-beam calculations. $|U_g||U_{h-g}||U_h|^{-1} = 2.3 \text{ \AA}^{-2}$. (b) Full three-beam calculations. $|U_g||U_{h-g}||U_h|^{-1} = 0.4 \text{ \AA}^{-2}$. (c) Calculations based on the second Bethe approximation. $|U_g||U_{h-g}||U_h|^{-1} = 2.3 \text{ \AA}^{-2}$.

(1982). The correspondence between the full calculations and the Bethe approximation for the weakest beam is very good apart from near the Bragg condition. For the stronger g beam the asymmetry in the full calculations is much smaller than for the h beam, and the Bethe results can in this case only be applied at large angles, as expected.

These results clearly demonstrate the applicability of the asymmetry-ratio method for determination of three-phase structure invariants, *i.e.* the phase invariant may in the general non-centrosymmetric case be determined by comparing the experimentally determined asymmetry ratios with profiles calculated for different structure-factor products. It should be stressed here, however, that this method is limited to the determination of the magnitude of the phase invariants. To distinguish between enantiomorphic forms the same type of many-beam effects can be used if the convergent-beam electron diffraction method is used (Goodman & Johnson, 1977).

As to the possible precision with which the phase invariants may be estimated, that depends strongly on the type of experiment used. But with an optimal experiment and proper intensity measurements, as for example the convergent-beam technique (Høier, Zuo, Marthinsen & Spence, 1988), precision of some degrees seems to be achievable.

An example

The asymmetry ratio $\eta(x)$ may in principle be extracted from any type of three-beam experiment. We shall here demonstrate one possibility, the selected-area channelling technique. The line contrast is here approximately proportional to the dispersion-surface gap width (*e.g.* Marthinsen & Høier, 1986), and the effective structure-factor ratio $\eta(x)$ may hence be found directly from experiments. The observed variation may then be compared with calculated profiles.

A theoretical example is shown in Fig. 5. In Fig. 5(a) calculated profiles are shown for the case given in Table 1, *i.e.* the 000, $3\bar{5}1$, $4\bar{4}\bar{2}$ three-beam case in GaP. The asymmetry ratio may be found by determining effective structure factors from profiles of the type $x = -a$ and $x = a$, where x is the distance from the line crossover. The line contrast, and hence effective structure factor for $\psi = 61^\circ$, for example, decreases for small and increasing positive x . For larger x it goes through a weak minimum and then increases again towards the two-beam value (Fig. 3).

$\psi = 0^\circ$ represents one of the possible centrosymmetric cases, and the calculated profile in Fig. 5(b) hence shows, as expected, the effect of zero effective structure factor for the weak beam, $4\bar{4}\bar{2}$. The corresponding zero contrast is seen within the encircled area in the figure. If ψ is taken to be 180° , this effect is found symmetrically at the other side of the crossover, *i.e.* for opposite signs of the excitation errors.

Concluding remarks

The effective structure factor, $|U_h^{\text{eff}}|$, and the associated dispersion-surface gap width are, as expected, found to depend strongly on the value of the three-phase structure invariant ψ . The degeneracy seen in the centrosymmetric case thus disappears rapidly with deviation from centrosymmetry. The inclusion of absorption in the diagonalization is not believed to have any important effect in this connection. The Bethe approximation is generally found to be good for the weakest beam apart from close to the simultaneous Bragg condition.

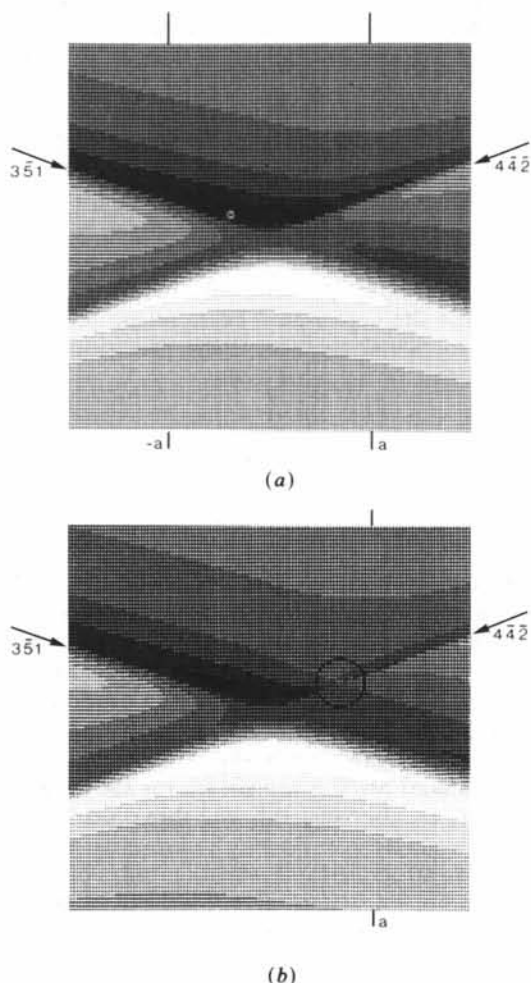


Fig. 5. Calculated channelling contrast for the 000, $3\bar{5}1$, $4\bar{4}2$ three-beam case in GaP. (a) $\psi = 61^\circ$; (b) $\psi = 0^\circ$.

The structure-factor asymmetry ratio η may in principle be determined from any type of three-beam experiments, e.g. convergent beam, channelling patterns, equal-thickness fringes, X-ray *Pendellösung*, X-ray single crystal or mosaic crystals. By comparison with theoretical profiles the magnitude of a large number of three-phase invariants may in such cases be determined from the observed intensities in the non-centrosymmetric case. These values may then be used as a starting set in the standard crystallographic programs.

In addition to the structure invariant, the ratio $\eta(x)$ depends on the excitation error of the coupled beam and on the structure-factor product $|U_g||U_{h-g}|/|U_h|$. The latter dependence shows, for example, that as a rule this effect is strongest in the weaker of the two coupled beams. Parameter dependences of this type may profitably be represented by calculated standard diagrams. Such calculations and applications using especially the convergent-beam technique will be published separately.

References

- CHANG, S. L. (1982). *Acta Cryst.* **A38**, 516-521.
 CHANG, S. L. (1986). *Phys. Rev. B*, **33**, 5848-5850.
 CHAPMAN, D., YODER, D. R. & COLELLA, R. (1981). *Phys. Rev. Lett.* **46**, 1578-1581.
 GJØNNES, J. (1981). *Fifty Years of Electron Diffraction*, edited by P. GOODMAN, pp. 408-432. Dordrecht: Reidel.
 GJØNNES, J. & HØIER, R. (1971). *Acta Cryst.* **A27**, 313-316.
 GOODMAN, P. & JOHNSON, A. W. S. (1977). *Acta Cryst.* **A33**, 997-1001.
 HØIER, R. & MARTHINSEN, K. (1983). *Acta Cryst.* **A39**, 854-860.
 HØIER, R., ZUO, J. M., MARTHINSEN, K. & SPENCE, J. C. H. (1988). Submitted to *Ultramicroscopy*.
 HÜMMER, K. & BILLY, H. (1982). *Acta Cryst.* **A38**, 841-848.
 HÜMMER, K. & BILLY, H. (1986). *Acta Cryst.* **A42**, 127-133.
 HUMPHREYS, C. J. (1979). *Rep. Prog. Phys.* **42**, 1825-1887.
 JURETSCHKE, H. J. (1982). *Phys. Lett. A*, **92**, 183-185.
 JURETSCHKE, H. J. (1986). *Acta Cryst.* **A42**, 449-456.
 KAMBE, K. (1957). *J. Phys. Soc. Jpn.* **12**, 13-25.
 MARTHINSEN, K. (1981). Thesis. Univ. of Trondheim-NTH, Norway.
 MARTHINSEN, K. & HØIER, R. (1986). *Acta Cryst.* **A42**, 484-492.
 MARTHINSEN, K. & HØIER, R. (1987). *Acta Cryst.* **A43**, C222.
 MARTHINSEN, K., MATSUHATA, H., HØIER, R. & GJØNNES, J. (1987). *Austr. J. Phys.* In the press.
 POST, B. (1979). *Acta Cryst.* **A35**, 17-21.
 POST, B. (1983). *Acta Cryst.* **A39**, 711-718.
 THORKILDSEN, G. (1987). *Acta Cryst.* **A43**, 361-369.
 THORKILDSEN, G. & MO, F. (1982). 7th Eur. Crystallogr. Meet., Jerusalem. Abstracts, p. 6.
 WOOLFSON, M. M. (1987). *Acta Cryst.* **A43**, 593-612.